CrossMark

ORIGINAL

Modelling and simulation of a moving interface problem: freeze drying of black tea extract

Ebubekir Sıddık Aydin[1] · Ozgun Yucel[1] · Hasan Sadikoglu[1,2]

Abstract The moving interface separates the material that is subjected to the freeze drying process as dried and frozen. Therefore, the accurate modeling the moving interface reduces the process time and energy consumption by improving the heat and mass transfer predictions during the process. To describe the dynamic behavior of the drying stages of the freeze-drying, a case study of brewed black tea extract in storage trays including moving interface was modeled that the heat and mass transfer equations were solved using orthogonal collocation method based on Jacobian polynomial approximation. Transport parameters and physical properties describing the freeze drying of black tea extract were evaluated by fitting the experimental data using Levenberg–Marquardt algorithm. Experimental results showed good agreement with the theoretical predictions.

List of symbols

C_{01}	Constant dependent only upon the structure of the porous medium and giving relative Darcy flow permeability (m²)
C_1	Constant dependent only upon the structure of the porous medium and giving relative Knudsen flow permeability (m)

✉ Ebubekir Sıddık Aydin
  e.aydin@gtu.edu.tr

  Ozgun Yucel
  yozgun@gtu.edu.tr

  Hasan Sadikoglu
  sadikoglu@gtu.edu.tr

1 Department of Chemical Engineering, Gebze Technical University, 41400 Gebze, Kocaeli, Turkey

2 Department of Chemical Engineering, Yildiz Technical University, 34210 Davutpaşa, Esenler, İstanbul, Turkey

C_2	Constant dependent only upon the structure of the porous medium and giving the ratio of bulk diffusivity (dimensionless)
C_p	Heat capacity (kJ/kg K)
C_{sw}	Concentration of bound (sorbed) water (kg water/kg solid)
$D^o_{w,in}$	$D_{w,in}P$ (N/s)
$D_{w,in}$	Free gas mutual diffusivity in a binary mixture of water vapor and inert gas
$f(T_X)$	Water vapor pressure–temperature functional form
k	Thermal conductivity
k_1	Bulk diffusivity constant, $C_2 D^o_{w,in} K_w/(C_2 D^o_{w,in} + K_{mx}P)$
k_2,k_4	Self-diffusivity constant, $(K_w K_{in}/(C_2 D^o_{w,in} + K_{mx}P)) + (C_{01}/\mu)$
k_3	Bulk diffusivity constant, $C_2 D^o_{w,in} K_{in}/(C_2 D^o_{w,in} + K_{mx}P)$
kd	Desorption rate constant of bound water
kf	Film thermal conductivity (kW/m K)
K_{in}	Inert gas Knudsen diffusivity, $K_{in} = C_1(RT_1/M_{in})^{0.5}$
K_{mx}	Mean Knudsen diffusivity for binary gas mixture, $K_{mx} = (y_w K_w + y_{in} K_{in})$
K_w	Water vapor Knudsen diffusivity, $K_w = C_1(RT_1/M_w)^{0.5}$
L	Thickness of being dried material (m)
M	Molecular weight (kg)
N	Mass flux ($N_w + N_{in}$)
P	Total pressure in dried layer (Pa)
q	Energy flux
R	Universal gas constant
t	Time
T	Temperature
V	Velocity of interface
X	Position of frozen interface
x	Space coordinate of distance along the height of the

material in the tray

Y   Mole fraction

Greek letters

ΔHs Enthalpy of sublimation of frozen water

ΔHv Enthalpy of vaporization of sorbed water

μ Viscosity

α Thermal diffusivity

ε_p Voidage fraction

ε Emissivity constant

ρ Density

σ Stefan–Boltzman constant

Superscripts

o   Initial value at t = 0

Subscripts

e   Effective value

exp   Experimental

f   Film

I   Dried layer

II   Frozen layer

in   Inert

L   Value at x = L

LP   Lower plate

m   Melting

mx   Mixture

o   Surface value

scor   Scorch

t   total

UP   Upper plate

w   Water vapor

x   Interfacial value

1 Introduction

Freeze drying known as "Lyophilization" is a key separation processes (the sublimation of frozen solvent (water) content from the material being dried) mainly used in pharmaceuticals, biotechnology, fine chemicals, and food industries. The conventional drying processes (evaporative drying, drum drying, spray drying, etc.) may cause loss of aroma, taste, texture, and nutrition utilize higher operation temperatures compared to the freeze drying. Thus, the highest quality products can be obtained by freeze drying compare to the conventional drying processes.

Freeze drying process consists of the preparation stages, freezing, primary drying stage, secondary drying stage, packaging, and storage. In order to keep prime properties (activity, stability, structure, flavor, taste, etc.) and obtain the finest quality products, each stage is critical and requires maximum care possible. Freeze-drying is a relatively expensive separation process
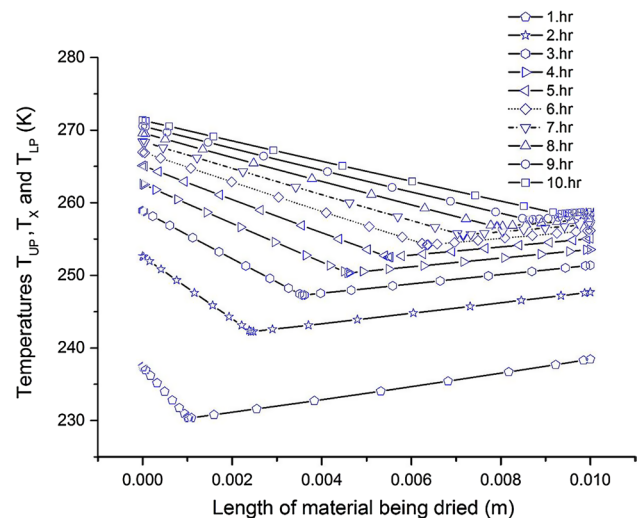
Fig. 1 Temperature distribution of T_{UP}, T_X and T_{LP} during primary drying stage

requiring long processing time and high energy demand. There are two stages in drying process; primary drying and secondary drying. To supply energy for vacuum and sublimation of frozen water, among the stages of freeze drying, the primary drying stage requires time and energy as compared to the other stages of freeze drying such as freezing and secondary drying stage [15]. Therefore, optimization of primary drying stage becomes crucial for the freeze drying process.

The freeze drying process fits perfect to the high market value products such as pharmaceuticals, fine chemicals, biotechnological products, and expensive foods. During drying, the water in the product changes its physical phase from solid to gas by sublimation. This process can be modeled as a moving interface while the product is drying. Duration of primary drying stage can be determined by estimating the position of moving interface.

Figure 1 shows a typical temperature distribution during the primary drying stage while the moving interface position changes. T_x, states the temperature of the moving interface is also the lowest point of the temperature profile during primary drying stage. The interface position approaches the length of the material until the primary drying stage of freeze drying has been completed. The heat and mass transfer mechanism of freeze drying stages has been extensively investigated in the literature [5, 9, 13, 16, 22]. In contrast, Sadikoglu et al. has constructed a mathematical model for skim milk. The best fit of heat and mass transfer coefficients to the experimental results of freeze drying of skim milk has been determined. Their mathematical model utilizes the dusty-gas model which does not require detailed information about the porous matrix structure of the dried layer [2, 6, 11, 12]. However, a detailed freeze drying of the black tea extract has not been investigated.
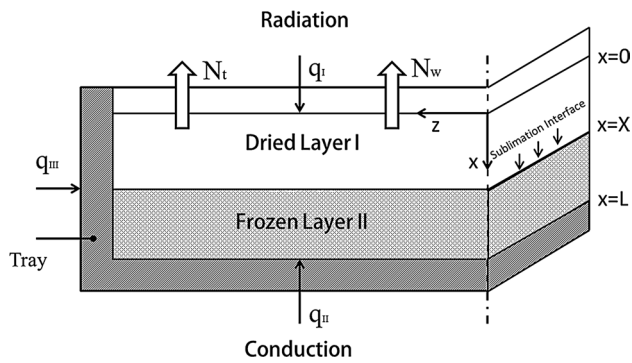
Fig. 2 Diagram of a material on a tray during freeze-drying [the variable X denotes the position of the sublimation between the freeze-dried layer (layer I) and the frozen layer (layer II)]

The orthogonal collocation method can be successfully applied to the solution of moving boundary problems in finite media. On the other hand, finite element analysis is also a successful method, however it could make a difficulty in applying moving boundary to the sublimation interface [1, 10]. An empirical and statistical approach using the response surface method gives a predicted property of the resultant dried product, but doesn't give the status of products during drying [3, 14].

In this study, the aim is to determine heat and mass transport parameters during freeze drying black tea extract. The equations associated with heat and mass transfer mechanisms established by [16] were used as the model equations, successfully transformed due to solve moving interface problem. Then the parameter estimation was accomplished by Levenberg–Marquardt minimization algorithm, also known as the damped least-squares (DLS) method is actually a combination of two minimization methods: the gradient descent method and the Gauss–Newton method. One dimensional mathematical model devised using conservation of mass and energy presented to describe dynamic behavior of drying stages of freeze drying of bulk solution of black tea extract in trays.

1.1 Mathematical model of freeze-dried black tea extract

The free water (frozen) and bound water (unfrozen) are removed from the material by sublimation occurs as a result of heat being conducted to the sublimation interface through dried layer I and frozen layer II. As shown in Fig. 2, the terms of N_t and N_w state the total mass flux and water vapor mass flux in dried layer. N_t is the sum of the mass flux of water and inert vapor gas. The q_I represents the heat input to the upper surface of dried layer of the product that is being freeze-dried by radiation, while q_{II} represent the heat input to the frozen bottom surface the material being freeze dried by conduction. The term q_{III} depicts the heat input to side

surfaces of the material being freeze dried but the top and bottom surfaces of the tray loaded by black tea extract are much larger than the side surfaces of the tray. The heat input from the side surfaces of the tray can be neglected throughout the calculation without introducing any significant error. The magnitude of q_I and q_{II} are altered by changing the upper and lower plate temperatures because freeze dryer designs do not allow to control the upper and lower plate temperatures independently. Thus, the heat input from the frozen bottom surface is always larger than the heat input from the dried top surface of the product.

1.1.1 Primary drying stages

During the primary drying stage, the heat required for sublimation of frozen water at interface that separates the dried and frozen layers, supplied by heating plates through dried (I) and frozen (II) layers by radiation and by conduction, respectively. In order to construct the mathematical model to represent primary drying stages of the freeze drying of black tea extract in tray, the following assumptions have been made:

- One dimensional heat and mass transfer modeled assumed to occur normal to the interface and surface,
- Sublimation occurs at an interface parallel to and at a distance X from the surface of the sample,
- The thickness of interface is taken to be infinitesimal,
- A binary mixture of water vapor and inert gas flows through the dried layer,
- The concentration of water vapor is assumed to be under equilibrium with the ice at the moving interface,
- Solid matrix and the gas has been assumed to be thermal equilibrium in the porous region,
- The frozen region is considered to be homogeneous, thermal conductivity, density and specific heat are assumed to be constant,
- The frozen region contains a negligible proportion of dissolved gas [8, 12].

The temperature distributions in dried (I) and frozen (II) layers, water vapor and inert concentration distributions in dried (I) region, can be determined using Eqs. 1–3 for dried (I) and frozen (II) layers.

$$\frac{\partial T_I}{\partial t} = \alpha_{Ie} \frac{\partial^2 T_I}{\partial x^2} - \frac{C_{pg}}{\rho_{Ie} C_{Ie}} \frac{\partial (N_t T_I)}{\partial x} + \frac{\Delta H_v \rho_I}{\rho_{Ie} C_{Ie}} \frac{\partial C_{sw}}{\partial t} \quad 0 \le x \le X \quad (1)$$

$$\frac{\partial T_{II}}{\partial t} = \alpha_{II} \frac{\partial^2 T_{II}}{\partial x^2} \quad X \le x \le L \quad (2)$$

$$\frac{1}{R} \frac{\partial}{\partial t} \left(\frac{P_w}{T_I} \right) = -\frac{1}{M_w \varepsilon} \frac{\partial N_w}{\partial x} - \frac{\rho_I}{M_w \varepsilon} \frac{\partial C_{sw}}{\partial t} \quad 0 \le x \le X \quad (3)$$

$$\frac{1}{R}\frac{\partial}{\partial t}\left(\frac{P_{in}}{T_I}\right) = -\frac{1}{M_{in}\varepsilon}\frac{\partial N_{in}}{\partial x} \quad 0 \leq x \leq X \tag{4}$$

The parameters water vapor mass flux, N_w and inert mass flux, N_{in} that appear in Eqs. (3) and (4), respectively can be determined by using the dusty-gas model:

$$N_w = -\frac{M_w}{RT_I}\left(k_1\frac{\partial p_w}{\partial x} + k_2 p_w\left(\frac{\partial p_w}{\partial x} + \frac{\partial p_{in}}{\partial x}\right)\right) \tag{5}$$

$$N_{in} = -\frac{M_{in}}{RT_I}\left(k_3\frac{\partial p_{in}}{\partial x} + k_4 p_{in}\left(\frac{\partial p_w}{\partial x} + \frac{\partial p_{in}}{\partial x}\right)\right) \tag{6}$$

The Eqs. (5) and (6) must be differentiated with respect to space coordinate x, before replacing them in Eqs. (3) and (4). One expression to describe the removal of the bound (unfrozen) water from the inside of the solid is based on the linear desorption rate of the bound water using a proper desorption rate constant [16]. In this work, we utilized the linear desorption rate equation to describe (removal) of bound water:

$$\frac{\partial C_{sw}}{\partial t} = -k_d C_{sw} \tag{7}$$

where k_d is the desorption rate constant. The initial and boundary conditions of Eqs. (1)–(6) and (7) are as follows:

$$T_I = T_{II} = T_x = T^0, \quad t = 0, \quad 0 \leq x \leq L \tag{8}$$

$$p_w = p_w^0, \quad p_{in} = p_{in}^0, \quad t = 0, \quad 0 \leq x \leq X \tag{9}$$

$$C_{sw} = C_{sw}^0, \quad t = 0, \quad 0 \leq x \leq L \tag{10}$$

$$q_I = -k_{Ie}\frac{\partial T_I}{\partial x}\bigg|_{x=0} \quad x = 0 \quad t > 0 \tag{11}$$

For dried layer I, heat transfer to the upper dried surface by radiation,

$$q_I = \sigma\varepsilon\left(T_{up}^4 - (T_I(t,0))^4\right) \quad t > 0 \tag{12}$$

The material and energy balances at infinitesimal thickness of interface result the following equation from where the temperature of interface can be determined.

$$q_{II} = -k_{II}\frac{\partial T_{II}}{\partial x}\bigg|_{x=L} \quad x = L \quad t > 0 \tag{15}$$

There is a thin film between the frozen material and lower surface of the tray and k_f is the thermal film conductivity coefficient.

$$q_{II} = k_f(T_{LP} - (T_{II}(t,L))) \quad t > 0 \tag{16}$$

P_o implies the sum of water vapor pressure (P_w) and inert gas pressure (P_{in}).

$$p_w = p_w^o \quad x = 0 \quad t > 0 \tag{17}$$

$$p_{in} = p_{in}^o = P_o - p_w^o \quad x = 0 \quad t > 0 \tag{18}$$

The variable p_w^o, is the chamber water vapor pressure, usually determined by the condenser design and assumed constant within the drying chamber. The variable P_o denotes the total pressure $\left(P_o = p_w^o + p_{in}^o\right)$ at $x = 0$, and is usually considered to be approximately equal to the total pressure in the drying chamber.

$$p_w = f(T_x) \quad x = X \quad 0 < t \leq t_{x=L} \tag{19}$$

$$\frac{\partial p_{in}}{\partial x}\bigg|_{x=X} = 0 \quad x = X \quad 0 < t \leq t_{x=L} \tag{20}$$

where V is the velocity of interface that is calculated by the mass flux of water vapor at interface (x = X) dividing of difference of frozen layer II density and equilibrium density at interface.

$$V = \frac{dX}{dt} = \frac{-N_w|_{x=X}}{\rho_{II}-\rho_I} \quad X = 0 \quad t = 0 \tag{21}$$

Minus sign at the in front of water vapor mass flux indicate the direction and it is the opposite direction of the moving interface velocity.

1.1.2 Secondary drying stage

The secondary drying stage starts at the end of the primary drying stage where the frozen free water content of the material is completely removed. This drying stage involves

$$k_{II}\frac{\partial T_n}{\partial x}\bigg|_{x=X} - k_{Ie}\frac{\partial T_I}{\partial x}\bigg|_{x=X} + V\left(\rho_{II}C_{pII}T_{II}|_{x=X} - \rho_I C_{pI}T_I|_{x=X}\right) + N_t C_{pg}T_x = -\Delta H_S N_t \quad \text{at} \quad x = X \text{ and } 0 < t \leq t_{x=L} \tag{13}$$

The interface temperature is also the right boundary condition of the frozen section and the left boundary condition of the dried section.

$$T_I = T_x = T_{II} \quad x = X \quad t > 0 \tag{14}$$

the removal of bound water from inside the sample resulted by physical and chemical adsorption, or crystallization [19]. During the secondary drying stage, the energy and material balance equations representing the temperature, phase pressures, and bound water concentration are same

equations those are derived in the primary drying stage. However, in this stage those equations are also to be solved for the varying thickness of the drying material. The resulting equation is shown in Eq. 22,

$$\frac{\partial T_I}{\partial t} = \alpha_{Ie} \frac{\partial^2 T_I}{\partial x^2} - \frac{C_{pg}}{\rho_{Ie} C_{Ie}} \frac{\partial (N_t T_I)}{\partial x} + \frac{\Delta H_v \rho_I}{\rho_{Ie} C_{Ie}} \frac{\partial C_{sw}}{\partial t} \quad 0 \leq x \leq L \quad (22)$$

Initial and boundary conditions for Eq. (22) are as follows:

$$T_I = \gamma(x), \, t = t_{x=L}, \, 0 \leq x \leq L \quad (23)$$

$$q_I = -k_{Ie} \left. \frac{\partial T_I}{\partial x} \right|_{x=0} \quad x = 0 \quad t > t_{x=L} \quad (24)$$

Heat transfer to the upper dried surface by radiation,

$$q_I = \sigma \varepsilon \left(T_{up}^4 - (T_I(t,0))^4 \right) \quad t > t_{x=L} \quad (25)$$

$$q_{II} = -k_{Ie} \left. \frac{\partial T_I}{\partial x} \right|_{x=L} \quad x = L \quad t > t_{x=L} \quad (26)$$

Initial and boundary conditions of Eqs. (2)–(3) and (5) for the second drying stage are as follows:

$$p_w = \delta(x) \quad t = t_{X=L} \quad 0 \leq x \leq L \quad (27)$$

$$p_{in} = \theta(x) \quad t = t_{X=L} \quad 0 \leq x \leq L \quad (28)$$

$$C_{sw} = v(x) \quad t = t_{X=L} \quad 0 \leq x \leq L \quad (29)$$

$$p_w = p_{wo} \quad p_{in} = p_{ino} = P_o - p_{wo} \quad x = 0 \quad t \geq t_{X=L} \quad (30)$$

$$\left. \frac{\partial p_w}{\partial x} \right|_{x=L} = 0 \quad x = L \quad t > t_{x=L} \quad (31)$$

$$\left. \frac{\partial p_{in}}{\partial x} \right|_{x=L} = 0 \quad x = L \quad t > t_{x=L} \quad (32)$$

$\gamma(x)$, $\delta(x)$, $\theta(x)$ and $v(x)$ are functions position, x and contain profile of T_I, p_w, p_{in}, and C_{sw}, obtained from the solution of the mathematical models at the end of the primary drying stage and they serve as initial conditions for the secondary drying stage. Immediately after the first dried layer come to existence during the primary drying stage, the secondary drying stage start taking place. But during the primary drying the concentration gradient between solid and dried pores is not significant. As a result the contribution of the removal of bound water to the total mass flux of the water removed during primary drying is not also significant. Subject to the physical properties of the material being freeze-dried, the secondary drying stage could be as long as the primary drying stage. Practically, 10–30% of the total water content of the material is removed by desorption during the secondary drying stage [19]. The required desorption heat

to remove the bound water molecules in the dried layer during the secondary drying stage is provided by the radiation from the top of the sample and by conduction from the bottom of the sample. Both heat inputs from top and bottom surfaces of the sample are transferred by the conduction throughout the porous dried layer [16, 17, 19].

2 Materials and methods

2.1 Materials

Çay Çiçeği black tea (produced by Çaykur) is a well-known and widely used trademark in Turkey used in this study. Commercial black tea extracted with distilled water, filtered then concentrated to 10% (w/w) in an evaporator under vacuum.

2.2 Freeze dryer

In freeze-drying experiments, the pilot scale freeze dryer (Virtis Ultra 25 XL, New York, NY) was used. The temperature of heating plates of the freeze dryer used in the drying experiment can be adjusted from −40 to 60 °C while the condenser temperature can be set as low as −70 °C. The four trays of the freeze dryer are capable to hold 25 L of solution. The condenser where sublimated and desorbed water vapor removed from the drying chamber by condensation has surface area of 3264 cm². The vacuum system of the freeze dryer equipped with one compressor with a power of 1.12 kW, and capable of supplying vacuum as low as 10 Pa.

2.3 Experimental verification

Five hundred grams of black tea was added into 5000 L of boiling distilled water in a steel container to allow soluble solids of black tea to infuse into boiling water. Solution filtered and concentrated to 10% (w/w) in an evaporator under vacuum. Concentrated 10% (w/w) 150 mL solution poured in the tray (0.10 m × 0.15 m × 0.04 m) of the freeze dryer. The heating plates temperature of the freeze dryer was set at −35 °C for 4 h to completely freeze the concentrated solution for each experiment. On completion of freezing, the drying chamber pressure was set to 10 Pa and kept constant during the drying. The air in the drying chamber evacuated by the vacuum pump in 30 min to reach set pressure of 10 Pa. Detailed information about freeze drying of black tea solution was not available in the literature, but it is known that the primary drying stage of freeze drying is a mass transfer controlled process while the secondary drying stage of freeze drying is a heat transfer controlled process. Therefore, the drying chamber pressure

Table 1 Freeze drying conditions of black tea extract

Freeze drying stage	Shelf temperature (°C)	Drying chamber pressure (Pa)
Freezing	−35	50
Primary freeze drying	+10	10
Secondary freeze drying	+30	10

was set to 50 Pa that is minimum value can reached for employed freeze dryer, well below the ice vapor pressure of the sample to increase water vapor mass flux through the pores of the dried material resulted by the sublimation during the primary drying stage [17, 18].

Moderately high chamber pressure could be beneficial for the heat transfer limited secondary drying stage by increasing the heat transfer capacity of the dried matrix, to facilitate the removal of bound water from the solid phase of the material being freeze dried. The problem is distinguishing the primary and secondary drying stages for freeze drying of black tea extract is almost impossible. Therefore, the drying chamber pressure was set its minimum value during both the primary and secondary drying stages. The heating plate temperatures of the freeze dryer and chamber pressures are given in Table 1. From the beginning to the end of the freeze-drying process, weight measurements were taken for every 2 h to obtain the weight loss of the samples.

2.4 Moisture content analysis

Certain amount of tea sample were placed into a pre-weighed dish and evaporated in an oven at 100 °C (± 2) for 24 h. Then sample was cooled in a desiccator and brought to constant weight. From the weight of residue, moisture content and the amount of total solids in the tea leaves were obtained.

2.5 Numerical solution of developed mathematical model

As mentioned before, the mathematical models that given in this work to represent dynamic behavior of both the primary and secondary drying stages of freeze drying of black tea extract in the tray solved by numerical techniques of orthogonal collocation that demands less computational time because it generates smaller problems [4]. In the primary drying, the Eqs. (1)–(4) along with the constitutive equations of water vapor and inert mass fluxes [Eqs. (5)–(6)], boundary [Eqs. (8)–(10)] and initial conditions [Eqs. (11)–(20)] are the set of nonlinear parabolic partial differential equations with moving boundary [Eq. (21)] and

requires simultaneous solution. Before using the orthogonal collocation method, all equations were put in dimensionless by defining dimensionless spatial direction for both the dried (I) and frozen (II) layers.

$$\xi = \frac{x}{X} \quad 0 \leq x \leq X \tag{33}$$

$$\eta = \frac{x - X}{L - X} \quad X \leq x \leq L \tag{34}$$

Then the transformed models are conveniently discretized using orthogonal collocation with the collocation points in the spatial direction. The trial functions chosen to be sets of orthogonal Jacobi polynomials [21] which satisfied the boundary conditions and the roots to the polynomials gave the collocation points. Thus, collocation points are taken as the roots of orthogonal Jacobi polynomials whose all roots are located between 0 and 1. The first and the second partial derivative with respect to dimensionless spatial direction can defined as follows:

$$\frac{\partial Y(i)}{\partial \xi} = \sum_{j=1}^{N+2} A(i,j)Y(i), \quad 0 \leq \xi \leq 1 \tag{35}$$

$$\frac{\partial^2 Y(i)}{\partial \xi^2} = \sum_{j=1}^{N+2} B(i,j)Y(i), \quad 0 \leq \xi \leq 1 \tag{36}$$

In Eqs. (35)–(36), ξ is the dimensionless spatial direction, Y represents dependent variable such as temperature of the dried layer T_I, temperature of the frozen layer T_{II}, water vapor pressure p_w, and inert pressure p_{in}, i represents root of orthogonal polynomial (collocation points) while A and B represent discretization matrices come from orthogonal collocation method. The roots of the Jacobi polynomials and discretization matrices of A and B for required number of collocation points were calculated by using the method developed by [23]. Employing discretization matrices of A and B for required number of collocation points, the energy balances in the dried (I) and frozen (II) layers and the material balances in the dried layer (I), become as follows:

$$\frac{\partial T_I(i)}{\partial t} = \frac{\alpha_{Ie}}{X^2} \sum_{j=1}^{N+2} B(i,j)T_I(i)$$

$$+ \frac{1}{X}\left(\xi(i)\frac{\partial X}{\partial t} - \frac{C_{pg}}{\rho_{Ie}C_{Ie}}\left(N_t(i)\sum_{j=1}^{N+2} A(i,j)T_I(i)\right.\right.$$

$$\left.\left. + T_I(i)\sum_{j=1}^{N+2} A(i,j)N_t(i)\right)\right)$$

$$+ \frac{\Delta H_v \rho_I}{\rho_{Ie}C_{Ie}}\frac{\partial C_{sw}}{\partial t} \quad 0 \leq \xi \leq 1 \tag{37}$$

$$\frac{\partial T_{II}(i)}{\partial t} = \frac{\alpha_{II}}{(L-X)^2} \sum_{j=1}^{N+2} B(i,j) T_{II}(j)$$
$$+ \frac{dX}{dt} \left(\frac{L(\eta-1) + X(1-\eta)}{(L-X)^2} \right)$$
$$\times \sum_{j=1}^{N+2} A(i,j) T_{II}(j) \quad 0 \le \eta \le 1 \tag{38}$$

$$\frac{\partial p_w(i)}{\partial t} = \frac{\xi(i)}{X} \frac{\partial X}{\partial t} \sum_{j=1}^{N+2} A(i,j) p_w(i)$$
$$- \frac{R T_I(i)}{\varepsilon_p M_w} \left(\frac{1}{X} \sum_{j=1}^{N+2} A(i,j) N_t(i) + \rho_{Ie} k_d C_{sw} \right) \quad 0 \le \xi \le 1 \tag{39}$$

$$\frac{\partial p_{in}(i)}{\partial t} = \frac{\xi(i)}{X} \frac{\partial X}{\partial t} \sum_{j=1}^{N+2} A(i,j) p_{in}(i)$$
$$- \frac{R T_I(i)}{\varepsilon_p M_{in}} \left(\frac{1}{X} \sum_{j=1}^{N+2} A(i,j) N_t(i) \right) \quad 0 \le \xi \le 1 \tag{40}$$

$$\frac{\partial C_{sw}(i)}{\partial t} = \frac{\xi(i)}{X} \frac{\partial X}{\partial t} \sum_{j=1}^{N+2} A(i,j) C_{sw}(i) - k_d C_{sw} \quad 0 \le \xi \le 1 \tag{41}$$

$$\frac{\partial X}{\partial t} = -\frac{N_w|_{\xi=1}}{\rho_{II} - \rho_I} \tag{42}$$

For all equation presented above i ($i = 1, 2, 3, …, N$) represents internal collocation points that corresponds to roots of the orthogonal Jacobi polynomials except 0 and 1. Index j ($j = 1, 2, 3, …, N + 2$) also represents the internal collocation points where $j = 1$ and $j = N + 2$ means the first and last collocation points that correspond the first and final root of the Jacobi polynomial that is 0 and 1, respectively.

Eventually, the partial differential equations that given in Eqs. (1)–(4) and (7), (21) are transformed to ordinary differential equations system [Eqs. (37)–(42)] with following initial and boundary conditions:

$$T_I|_{\xi=0} = T_I|_{\xi=1} = T_{II}|_{\eta=1} = T^0 \quad t = 0 \quad 0 \le \xi \le 1 \tag{43}$$

$$p_w = p_w^0 \quad t = 0 \quad 0 \le \xi \le 1 \tag{44}$$

$$p_{in} = p_{in}^0 \quad t = 0 \quad 0 \le \xi \le 1 \tag{45}$$

$$C_{sw} = C_{sw}^0 \quad t = 0 \quad 0 \le \xi \le 1 \tag{46}$$

$$T|_{\xi=0} = \frac{-k_{Ie} \sum_{j=2}^{N+2} A(1,j) T_I(j) - X\sigma F_{up} \left(T^4 \big|_{\xi=0} - T_{up}^4 \right)}{k_{Ie}(A(1,1))} \tag{47}$$

$$T_I|_{\xi=1} = T_{II}|_{\eta=1}$$
$$= \frac{\frac{k_{Ie}}{X} \left(A(N+2,1) T_I|_{\xi=0} + \sum_{j=2}^{N+1} A(N+2,j) T_I(j) \right) - \Delta H_s N_t|_{\xi=1}}{N_t|_{\xi=1} \left(C_{pg} - \frac{\rho_{II} C_{pII} - \rho_I C_{pI}}{\rho_{II} - \rho_I} \right) - \frac{k_{Ie}}{X} A(N+2, N+2)} \tag{48}$$

$$T_{II}|_{\eta=1} = \frac{\frac{k_{II}}{L-X} T_X + k_f T_{LP}}{\left(\frac{k_{II}}{L-X} + k_f \right)} \tag{49}$$

$$p_w = p_w^o \quad \xi = 0 \quad t > 0 \tag{50}$$

$$p_{in} = p_{in}^o = P_o - p_w^o \quad \xi = 0 \quad t > 0 \tag{51}$$

$$p_w = f\left(T|_{\xi=1} \right) \quad \xi = 1 \quad t > 0 \tag{52}$$

$$p_{in}|_{\xi=1} = -\frac{\sum_{j=1}^{N+1} A(N+2,j) p_{in}(j)}{A(N+2, N+2)} \quad \xi = 1 \quad t > 0 \tag{53}$$

The initial condition for Eq. (42) is X = 0.0001 at t = 0, but this means that there exist dried layer at the beginning of freeze drying, this not realistic but it required for the numerical solution. In the secondary drying stage, there is no moving boundary and froze (II) layer. Therefore, Eq. (38) totally eliminated and X is set to L while derivative of X is set equal zero to obtain numerical solution for the secondary drying stage.

2.6 Algorithm of numerical solution

Time dependent ordinary and partial differential equations for freeze drying process are complex to simulate the process. In order to solve the models equations, explicit and implicit approaches are used. While the explicit method calculates the state of a system at a later time from the state of the system at the current time, the implicit method solves an equation involving both the current state and later state of the system [20]. The expressions of explicit and implicit methods are given below, respectively. Mathematically, t denotes the current system state and $t + \Delta t$ denotes the state at later time.

$$T(t + \Delta t) = F(T(t)) \tag{54}$$

$$F(T(t), T(t + \Delta t)) = 0 \tag{55}$$

Equation (55) is implicitly solved to find $T(t + \Delta t)$. As shown from Eq. (55), although implicit form involves extra term and requires extra a computational effort, it uses larger time steps and takes less computational time. In our study, the model equations transformed to the implicit form like Eq. (55) and it was seen from the numerical analysis, implicit approach is more suitable for the our model equations. The ode15i Matlab solver was used to solve our model and all equation transformed fully implicit form as:

$$F\big(t, y(t), y'(t)\big) = 0 \qquad (56)$$

There are novelties because there are two Jacobian matrices, dF/dy and dF/dy' that can be given manually; also solver can estimate approximate Jacobian. Specific vectorized format is needed for the ode15i Matlab solver, in the present model all equation vectorized [like Eq. (57)] and solved simultaneously.

$$if \quad y'(t) = G(t) => 0 = y'(t) - G(t) \qquad (57)$$

Orthogonal collocation uses collocation at the zeros of some orthogonal polynomial (Jacobi polynomial for this work) to transform the partial differential equation (PDE) to a set of ordinary differential equations (ODEs). In our system, to describe the dynamic behavior of the primary drying stage, there are 5 PDEs (Eqs. 1–4, 7) and 1 ODE [Eq. (21)]. With the A and B matrices which are difference operators established by collocation method, our PDE equations can be easily converted ODEs that shown before (Eqs. 37–42). Then 5n + 1 ODE equations are solved with ode15i solver.

The solution algorithm is:

Step 1   Determine n, the number of collocation points in axial direction. Set initial data: $T_I = T_{II} = T_x = T^0, p_w = p_w^0, p_{in} = p_{in}^0, C_{sw} = C_{sw}^0$ and set initial time interval for ode15i.

Step 2   Calculate position of collocation points r_1, r_2 vectors and difference operators A and B matrices using the methods described by Villadsen and Michelsen (Collocation points r_1 and r_2 represent ξ and η respectively).

Step 3   Calculate heat and mass transfer parameters (ρ_1, ρ_2, Cp_1, Cp_2, k_1, k_2).

Step 4   Compute $T_I, T_{II}, T_x, p_w, p_{in}$ and C_{sw} for $t = t_{old} + \Delta t$ by solving the nonlinear algebraic system using ode15i solver.

Step 5   If the relative error of two iterates is less than a prescribed tolerance, stop the iteration and set new time interval go back to Step 4. Otherwise, save data at prescribed time intervals, set new time interval. Check whether the stopping criterion (X (t) = L) is met. If not then go to the Step 3 otherwise (T = T_{II}) and go to the Step 6.

(Please note that frozen and dried are solved in ξ and η domain respectively. Interior points positions can be calculated for frozen and dried part x = $X\xi$ and x = $\eta(L - X) + X$) respectively).

Step 6   Compute T, p_w, p_{in} and C_{sw} for specific time interval by solving the secondary drying equation set with ode15i solver.

Step 7   If the relative error of two iterates is less than a prescribed tolerance, stop the iteration and set new time interval go back to Step 6. Otherwise, check water vapor mass flux N_w. If the product is dried stop the iteration, otherwise set new time interval go back to Step 6.

3 Result and discussion

The theoretical results for the freeze drying of black tea extract were obtained by solving simultaneously Eqs. (37)–(42) with the initial and boundary conditions that given in from Eqs. (43)–(53) for primary drying stage. The numerical solution for the secondary drying stage obtained by eliminating Eq. (38) and (42) and setting X equal to L, also setting the derivative of X to equal because there is no frozen (II) layer or no moving interface. The values of the parameters as well as the expressions employed in the evaluation of certain parameters of the theoretical model are presented in Tables 2 and 3. The melting T_m and scorch T_{scor} temperatures of black tea extract chosen to be −10 and 40 °C, respectively.

In this work, the dynamic behavior of the removal of bound water was presented with the first-order rate desorption mechanism that given in Eq. (7). Detailed model calculations performed in this work have indicated that the total mass flux of the water removed during primary drying mainly resulted by sublimation of free water at interface, the contribution of the removal of bound water is limited. The result is in agreement with work of [16], therefore, the mechanism of the removal of bound water in the mathematical model during primary drying can be neglected without introducing a significant error.

3.1 Parameter estimation

The freeze drying of skim milk model developed by [16]. In their work, they considered freeze drying of skim milk in the sense that it can be acknowledged as a complex pharmaceutical product because it contains enzymes and proteins. Compared to freeze drying of black tea extract with skim milk, the ice crystals formed during the freezing stage that determines the size and shape of the pores, the pore size distribution, and the pore connectivity of the porous network of the dried layer formed by the sublimation of

Table 2 Parameters and values for freeze drying model of black tea extract

Parameters	Units	Values
kd_I	s^{-1}	6.48×10^{-7} (*during primary drying stage*)
L	m	0.01
p_{in}^o	N/m^2	8.93
p_w^o	N/m^2	1.07
P_0	N/m^2	10
T°	K	238.15
T_{LP}	K	283.15
T_{UP}	K	283.15
T_m	K	263.15
T_{scor}	K	313.15
f(Tx)	N/m^2	$133.3224[exp(-2445.5646/Tx + 8.2312l \log 10(Tx) - 0.01677006Tx + 1.20514 \times 10^{-5}Tx^2 - 6.757169)]$
ΔH_s	kj/kg	2840.0
ΔH_v	kj/kg	2687.4
ρ_{le}	kg/m^3	215.0
ρ_l	kg/m^3	212.21
ρ_{II}	kg/m^3	1018.0
σ	kW/m^2K	5.676×10^{-11}
ε		1

Table 3 Estimated model parameters

Parameters	Units	Values
C_{0l}	m^2	5.02×10^{-15}
C_2		0.921
Cp_g	kJ/kg K	0.9251
Cp_{le}	kJ/kg K	13.97
Cp_{II}	kJ/kg K	1.387
C_{sw}^o	kg water/kg solid	0.6415
$D_{w,in}^o$	$kg \, m/s^3$	$7.5667 \times 10^{-4}(T(x=0) + T(x=X))^{1.5})$
K_w	m^2/s	$1.2823 \times 10^{-4}(T(x=0) + T(x=X))^{0.5}$
K_{in}	m^2/s	$2.1685 \times 10^{-4}(T(x=0) + T(x=X))^{0.5}$
k_f	kW/m^2K	0.00873
k_{le}	kW/mK	$3.8467 \times 10^{-7}(Pin + P(x=X)) + 5.8975e^{-5}$
k_{II}	kW/mK	0.00043
kd_{II}	1/s	1.1505×10^{-4}
ε_p		0.749

frozen water during the primary drying stage, could be substantially different.

That means the parameter of the dusty gas model (water vapor Knudsen diffusivity, K_w, inert gas Knudsen diffusivity, K_{in}, along with the free gas mutual diffusivity in a binary mixture of water vapor and inert, $D_{w,in}$, and film thermal conductivity, k_f should be determined for freeze drying of black tea extract in tray. Parameters estimation done by searching the best-fit transport properties of the dried layer and the film thermal conductivity between heating plate and bottom surface of the tray, during freeze drying of black tea extract. In order to achieve this task, an iterative computation procedure is employed. For each iteration, if the difference between experimental data and computed data that obtained by solving dynamic mathematical model, is high, the initial guess of parameters was altered until the difference is minimum [7]. This procedure identical to the nonlinear least-square method where the sum of the square of the error that defined as difference between experimental data, y_{ex}, and theoretical data, y_t, minimized to obtain best fit values of the parameters.

$$SSE = \sum_{i=1}^{N} (y_{ex} - y_t)^2 \qquad (57)$$

In Eq. (57) N denotes number of the experimental data while i is the index (i = 1, 2,…N). Levenberg–Marquardt algorithm requires initial guesses and range (maximum and minimum tolerable values) for the parameters, given input data (y_{ex}) and observed output data (y_t) to perform parameter estimation. Both the given input data and observed output data must be the same size matrices or vectors. In this work, the given input data is the experimental amount of removed water that measured for every two hours starting at the beginning to end of the experiments. The observed output data calculated for the same time span of the given input data, by solving dynamic mathematical model that presented in this work. Nonlinear least-square algorithm continuously try to minimize the sum of square of error (SSE) between the given input data and observed output data, by adjusting the parameters in the given range. The parameters that give the minimum value of the SSE, are considered to be the best-fitted parameters of the dynamic mathematical model.

The estimated transport parameters shown in Table 3 can be used to reveal the heat and mass mechanisms involved in the freeze drying process. The structure of the porous matrix of the dried layer is very complex in order to model. Therefore the dusty gas model was used to describe mass transport in black tea extract. The structural parameters C_{01}, C_1 and pair of C_2, $D_{w,in}$ characterize the mechanism of intra-particle convective flow, and they used in calculation of self-diffusivity constant, Knudsen diffusivity and bulk diffusivity constant, respectively (detailed information can be seen in nomenclature). The diffusivity values are directly related to the pore structures of the materials. Knudsen diffusivity is important when the average free path of the gas molecules is greater than the pore diameter
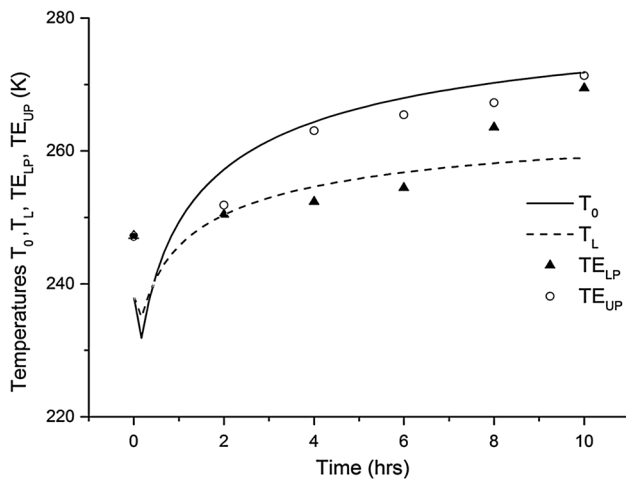
Fig. 3 The time variation of the theoretical top surface, T_0, theoretical bottom surface, T_L, experimental top surface TE_{UP} and experimental bottom surface TE_{LP}, temperatures during the primary drying stage

of the porous material and plays an effective role in the diffusion phenomena occurring in the porous materials.

3.2 Evaluation of simulated results

During primary drying stage, the theoretical and experimental temperature distributions on upper plate and lower plate against time were shown in Fig. 3. At the beginning of the primary drying stage frozen sample temperature is $T_F = 238.15$ K at x = 0 and drying heat treated to upper and lower surface by radiation and conduction, shelf temperature was 283.15 K. It is obvious that sudden temperature drop at first as a result of sublimation under the vacuum condition and higher temperature difference between the product surface and shelf temperature. The amount of heat required for sublimation enthalpy ΔH_S was obtained from this sudden temperature drop. TE_{UP} and TE_{LP} increased with time and at the end of the primary drying stage (t = 10 h) it is observed that temperatures of TE_{UP} and TE_{LP} were almost equal. The reason that moving sublimation interface ended its downward movement and primary drying stage was completed and secondary drying stage started. The downward movement of interface caused porous rigid structures in dried layer and amount of free water in porous rigid structures decreased with time. In other words, amount of heat required for sublimation is less that at the beginning and that causes temperature differences between upper plate and lower plate.

Figure 4 shows that theoretical results for mass flux of water vapor, $N_w \big|_{x=0}$ evaluated at the top surface of material being dried at various drying times during the primary drying stage. As shown from Fig. 3, initial water vapor mass flux rate is maximum value due to the
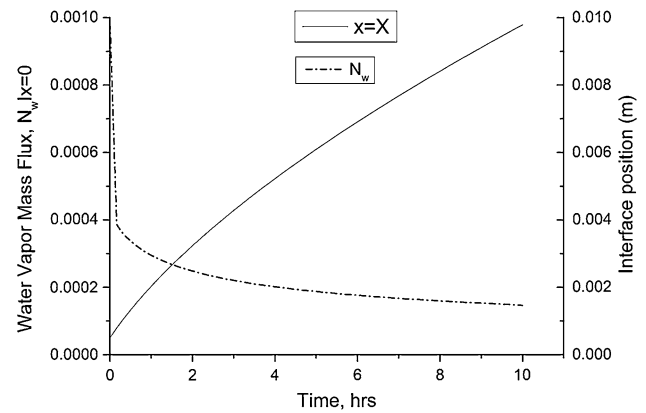
Fig. 4 The time variation of the water vapor mass flux, Nw $\big|$ x = 0, during the primary drying stage
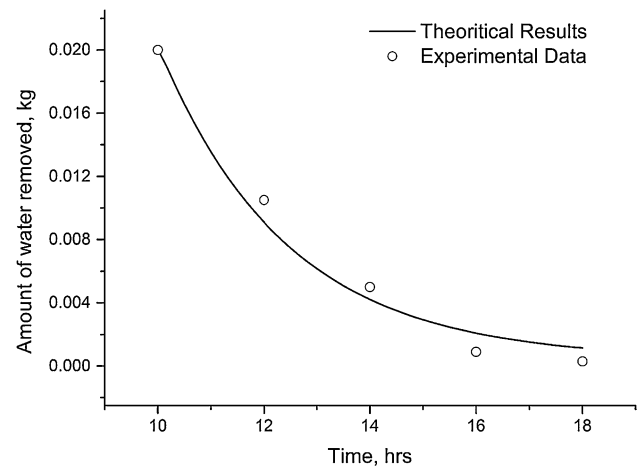
Fig. 5 Amount of residual water versus time during the secondary drying stage of the freeze-drying of instant tea

thickness of dried layer is almost infinitesimal and resistance to mass transfer may be ignored. As the primary drying stage proceeds porous dried layer is occurred by the moving sublimation interface and the porous dried layer provides a significant resistance to mass and heat transfer.

Figure 5 represents experimental data and the theoretical results for the amount of water removed in the sample at various drying times during the secondary drying stage. The mechanisms of mass transfer of water vapor and inert gas in the pores of the dried layer consider Knudsen diffusion, bulk diffusion, and convective flow. It should be noted again at this point that during the secondary drying stage, the water vapor in the pores of the dried layer is formed from the removal of bound (unfrozen) water from the phase of the solute (instant tea). Therefore, the contribution of the removal of bound water to the total mass

flux of water removed during the secondary drying stage is dominant, and the value of the k_d in Fig. 5 is two order of magnitude larger than the value of the k_d, during the primary drying stage (Table 2). This result clearly indicates mass transfer occur as a result of desorbing bound water from the phase of the solute, during the secondary drying stage. Further analyzing the profile in Fig. 4, the agreement between the experimental and the theoretical data is, for all practical purposes, good. During the secondary drying stage, the major mass transfer mechanisms are removal of bound water from the phase of the solute, Knudsen diffusion, bulk diffusion and the convective flow, for the freeze drying of black tea extract that studied in this work.

The three major mass transfer mechanisms during secondary drying were as follows: (I) removal of bound water from the phase of the solute, (2) Knudsen diffusion, and (3) bulk diffusion. In general, it is recommended that the mechanism of convective flow should be included in the mathematical model used to describe the dynamic behavior of the secondary drying stage, since one, for a given system of interest, cannot accurately estimate a priori the effect of the contribution of the convective flow on the drying rate during secondary drying; if, of course, numerous comparisons of theoretical results with experimental data from the system of interest indicate that the contribution of the mechanism of convective flow in the pores of the dried material is not significant during secondary drying, then one could neglect the mechanism of convective flow in the mathematical model used to describe the dynamic behavior of the secondary drying stage.

4 Conclusion

We constructed a mathematical model for freeze drying of black tea extract and transformed space due to moving interface. Thus, orthogonal collocation method is applied which involving transformations of PDEs to ODEs. In the solution of model equations, ODEs were adjusted in an implicit form and it is prior to solve the moving interface problems which are relatively stiffness. Using A and B discretization matrices come from orthogonal collocation and solving implicitly model equations enable to simulate the dynamic behavior of the processes accurately and with less effort. The estimated transport parameters that are difficult to measure directly can be used to predict the duration of freeze drying of black tea extract and reduce processing time and energy consumption in the next studies.

References

1. Ferguson WJ, Lewis RW, Tömösy L (1993) A finite element analysis of freeze-drying of a coffee sample. Comput Methods Appl Mech Eng 108:341–352
2. Gloor PJ, Crosser OK, Liapis AI (1987) Dusty-gas parameters of activated carbon absorbent particles. Chem Eng Commun 59:95–105
3. Hammami C, René F (1997) Determination of freeze-drying process variables for strawberries. J Food Eng 32:133–154
4. Hernández-Calderón OM, Rubio-Castro E, Rios-Iribe EY (2014) Solving the heat and mass transfer equations for an evaporative cooling tower through an orthogonal collocation method. Comput Chem Eng 71:24–38
5. Hottot A, Andrieu J, Vessot S, Shalaev E, Gatlin LA, Ricketts S (2009) Experimental study and modeling of freeze-drying in syringe configuration. Part I: freezing step. Dry Technol 27:40–48
6. Jackson R (1977) Transport in porous catalysts. Elsevier Scientific Pub. Co., Distributors for the U.S. and Canada, Elsevier North-Holland, Amsterdam, New York, New York
7. Kuu W-Y, McShane J, Wong J (1995) Determination of mass transfer coefficients during freeze drying using modeling and parameter estimation techniques. Int J Pharm 124:241–252
8. Liapis AI, Bruttini R (1994) A theory for the primary and secondary drying stages of the freeze-drying of pharmaceutical crystalline and amorphous solutes: comparison between experimental data and theory. Sep Technol 4:144–155
9. Liapis, A. I., Bruttini R.. (1995). Freeze Drying. In M. D. Mujumbar S.A. (Ed.), Handbook of Industrial Drying 2nd ed. (pp. 309-343). Newyork, Basel
10. Mascarenhas WJ, Akay HU, Pikal MJ (1997) A computational model for finite element analysis of the freeze-drying process. Comput Methods Appl Mech Eng 148:105–124
11. Mason EA, Malinauskas AP (1983) Gas transport in porous media: the dusty-gas model. Elsevier, New York
12. Millman MJ, Liapis AI, Marchello JM (1985) An analysis of the lyophilization process using a sorption-sublimation model and various operational policies. AIChE J 31:1594–1604
13. Muzzio CR, Dini NG (2011) Simulation of freezing step in vial lyophilization using finite element method. Comput Chem Eng 35:2274–2283
14. Nakagawa K, Ochiai T (2015) A mathematical model of multi-dimensional freeze-drying for food products. J Food Eng 161:55–67
15. Patel SM, Doen T, Pikal MJ (2010) Determination of end point of primary drying in freeze-drying process control. Aaps Pharmscitech 11:73–84
16. Sadikoglu H, Liapis AI (1997) Mathematical modelling of the primary and secondary drying stages of bulk solution freeze-drying in trays: Parameter estimation and model discrimination by comparison of theoretical results with experimental data. Dry Technol 15:791–810
17. Sadikoglu H, Liapis AI, Crosser OK (1998) Optimal control of the primary and secondary drying stages of bulk solution freeze drying in trays. Dry Technol 16:399–431
18. Sadikoglu H, Ozdemir M, Seker M (2003) Optimal control of the primary drying stage of freeze drying of solutions in vials using variational calculus. Dry Technol 21:1307–1331
19. Sadikoglu H, Ozdemir M, Seker M (2006) Freeze-drying of pharmaceutical products: research and development needs. Dry Technol 24:849–861
20. Shampine LF (2007) Design of software for ODEs. J Comput Appl Math 205:901–911

21. Solsvik J, Jakobsen HA (2012) Effects of Jacobi polynomials on the numerical solution of the pellet equation using the orthogonal collocation, Galerkin, tau and least squares methods. Comput Chem Eng 39:1–21

22. Song CS, Nam JH, Kim CJ, Ro ST (2002) A finite volume analysis of vacuum freeze drying processes of skim milk solution in trays and vials. Dry Technol 20:283–305

23. Villadsen J, Michelsen ML (1978) Solution of differential equation models by polynomial approximation. Prentice-Hall, New York